Lake basin development in the Holocene and its impact on the sedimentation dynamics in a small lake (southern Estonia)

Jaanus Terasmaa

Institute of Ecology, Tallinn University, Uus-Sadama 5, 10120 Tallinn, Estonia; jaanus.terasmaa@tlu.ee

Received 6 January 2011, accepted 25 April 2011

Abstract. Small lakes and their sediments are widely used for palaeolimnological reconstructions. Often only one core from the deepest part of the lake is used for reconstructing the lake catchment development, water-level changes and climate. To interpret palaeoinformation correctly, it is necessary to understand the spatio-temporal dynamics and the essence of lake basin evolution (topography, sedimentation zones, etc.) during the selected time period. The current study focuses on reconstructing the development of Lake Väike Juusa (southern Estonia) during the Holocene with the help of 3D digital elevation models compiled for the palaeolake stages at 9000 BP, 8000 BP, 4000 BP, 2000 BP and the present. The results suggest that we have to consider lake stages as completely different lakes with different sedimentation patterns – the hypsocraphic curve of Lake Väike Juusa was convex at the beginning of the Holocene and is concave nowadays. The proportion of the accumulation areas varied from 6% to 60% at the beginning of the Holocene and is around 30% nowadays. In order to understand lake basin development and water-level changes, the sampling sites should be selected close to the transitional zone and more than one core from a lake is needed. Commonly the sites located spatially rather close to each other have significantly different sedimentation patterns. Three-dimensional digital elevation models of palaeolake basins are useful tools for visualizing data and for hypothesizing about possible effects of lake-level fluctuations on the lake and its sedimentation regime.

Key words: water-level fluctuations, lake sediments, lake basin topography, sedimentation pattern, grain size, 3D digital elevation model.

INTRODUCTION

The spatial distribution, composition and texture of lake sediments reflect a complex interaction between catchment characteristics (topography, composition of deposits, vegetation, etc.), in-lake processes (thermal stratification, hydrological regime, effect of the lake biota, etc.) and morphology of the lake basin (topography of the basin and sediment surface, shape and size of the lake, etc.) (Gilbert 2003). Large-scale changes in lake sediments can be related to the hydrological balance, which in turn is driven by changes in climatic conditions and infiltration properties of the lake basin.

Water-level fluctuations and their impact on the sedimentation environment have been studied in many lakes over different timescales (Digerfeldt 1986; Tarasov & Harrison 1989; Dearing 1997; Eronen et al. 1999; Ojala & Saarinen 2002; Magny et al. 2003; Punning et al. 2007b). Past lake-level changes can be reconstructed most accurately by examining different types of complementary litho- and biostratigraphical evidence (Hannon & Gaillard 1997; Nesje & Dahl 2001; Snowball et al. 2002; Punning et al. 2005a, 2005b; Kangur et al. 2009). Since the mineral component of lake sediments is rather inert and is not easily affected by post-sedimentary processes, the grain size distribution of the sediment is widely used for this purpose (Boyle 2001; Last 2001). During the infilling of a lake with a constant area, the deposits are distributed over a continuously increasing area as the zone of accumulation progressively expands in response to infilling. If we assume that the yearly production remains constant, every year a thinner sediment layer is deposited (Davis & Ford 1982), thus providing a basis for delimiting areas of different sedimentation regimes (Lehman 1975; Håkanson & Jansson 1983; Blais & Kalff 1995; Richard et al. 2001; Yang et al. 2002). The mean grain size of mineral deposits decreases with increasing distance from the shore (from which the sediment is supposed to originate), so the mean size and sorting of the sediments at a given point in an extensive deposit provide measures of the local sorting of the deposit (Allen 1985). Therefore the sedimentary signals for lake-level changes in small closed lakes are more easily found in marginal sediments, which are sensitive to fluctuating lake levels in a variety of ways.

Previous detailed studies of Lake Väike Juusa (hereafter Lake Juusa) have enabled us to reconstruct the water-level fluctuations and their impact on biogeochemical cycling in the lake (Punning et al. 2003, 2004, 2005b; Koff et al. 2005; Terasmaa 2005a, 2005b, 2009; Punning & Puusepp 2007). These data serve as a reliable basis for constructing models of the sedimentation environment during the Holocene and provide a means for studying the relationships between the sediment characteristics and bottom topography during single periods within transgressive–regressive cycles. For this purpose we need to take into consideration changes in the lake basin topography and sedimentation zone by using the existing sediment core data and models developed for present-day sediment distribution.

The main aim of the current study is to determine the development of the Lake Juusa basin and spatio-temporal dynamics of the sedimentation environment, using the 3D digital elevation models compiled for the palaeolakes at 9000 BP, 8000 BP, 4000 BP, 2000 BP and the present. On the basis of 3D digital elevation models it is possible to describe lake basin development in a more precise way, delimit sedimentation zones from different periods and gain new knowledge about causes and consequences during lake evolution in the Holocene. The well-studied Lake Juusa is a good example for understanding the scale of the spatio-temporal changes occurring in the lake during its development.

STUDY AREA

Lake Juusa (58°03′33″N, 26°30′60″E) is a NE–SW oriented, small, closed hard-water lake, situated in the Otepää Heights in southern Estonia (Fig. 1A, B). The maximum length and width of this 3 ha lake are 250 and 160 m, respectively (Fig. 1B); the mean depth is 3.7 m and the maximum depth 6.0 m (Terasmaa 2005b). Lake Juusa is a meso-eutrophic dimictic lake with strong stratification during spring and summer (Punning et al. 2005a). During summer the thermocline deepens from about 2.5 m in June to 3–3.5 m in July–August.

Lake Juusa is characterized by a concave hypsographic curve (approximately 70% of the total water mass in the lake is in the epilimnetic zone) and a very small dynamic ratio (DR = 0.04) (see Håkanson & Jansson 1983). The lake bottom has a relatively regular shape, though the nearshore zone deepens abruptly. The lake bottom inclinations are greatest (up to 20%) at depths of 0 to 3 m and decrease rapidly with depth, being on average only 2% at depths below 5 m.

The catchment of Lake Juusa (55 ha) lies 122–170 m above sea level. The lake is surrounded by a terrace roughly 2 m higher than the present lake level. The hillocks that border the lake were formed from glacial deposits (till). The main soil types around the lake are Calcaric Cambisols, Calcaric Luvisols and Eutric Luvisols (Reintam 1995).

The climate in the area is continental, with cold winters and warm summers. The mean summer temperature is 16.5 °C and the mean winter temperature is –6 °C. The mean annual precipitation is about 650 mm (Jaagus & Tarand 1988).

The lake is situated in a semi-open cultural landscape (50% forest, 23% natural grassland). Spruce forest dominates on its northern slopes, while pine and/or deciduous trees dominate on the southern slopes. Cultivated grassland is dominant on the northern and southern sides of the lake. In the west the lake is bordered by a small paludified area occupying around 1% of the catchment.

The bottom sediments of Lake Juusa are over 10 m thick in the deepest part of the lake (Fig. 1C). The surface sediments in the accumulation area consist of brownish gyttja rich in water (on average 90%). The organic material content is on average 30%, and silt and clay fractions dominate in the basal layers of the sediment cores (Punning et al. 2005a).

MATERIAL AND METHODS

Fieldwork

The bathymetry of Lake Juusa was measured and mapped from a boat in summer and from the ice in winter. To measure the bathymetry, an echo sounder (Humminbird 100SX) and a Secchi disk 10 cm in diameter were used. The depth was measured at 174 locations with the Secchi disk, and the echo sounder was used to measure the lake-bottom topography. The locations of the sampling sites were recorded with GPS Garmin 12 (maximum horizontal accuracy 3 m) and a measuring tape.

To describe the sediment and map the lake basin topography, a piston corer was used. In addition, eleven sediment cores covering full sediment sequences were taken from ice with a Belarus (Russian) peat sampler. The cores were taken continuously, described in the field and then packed into bisected tubes for transportation. The samples remained refrigerated in the dark and sub-sampling was carried out in the laboratory prior to analysis. Nineteen surface sediment samples (up to 10 cm of sediment depth) (Fig. 1) were taken with a gravity corer modified by the Institute of Ecology. The sediment samples were packed in the field into hermetic PVC boxes and refrigerated until analysis. The data obtained from the surface sediment samples analysis have been published in Terasmaa (2005a, 2005b).

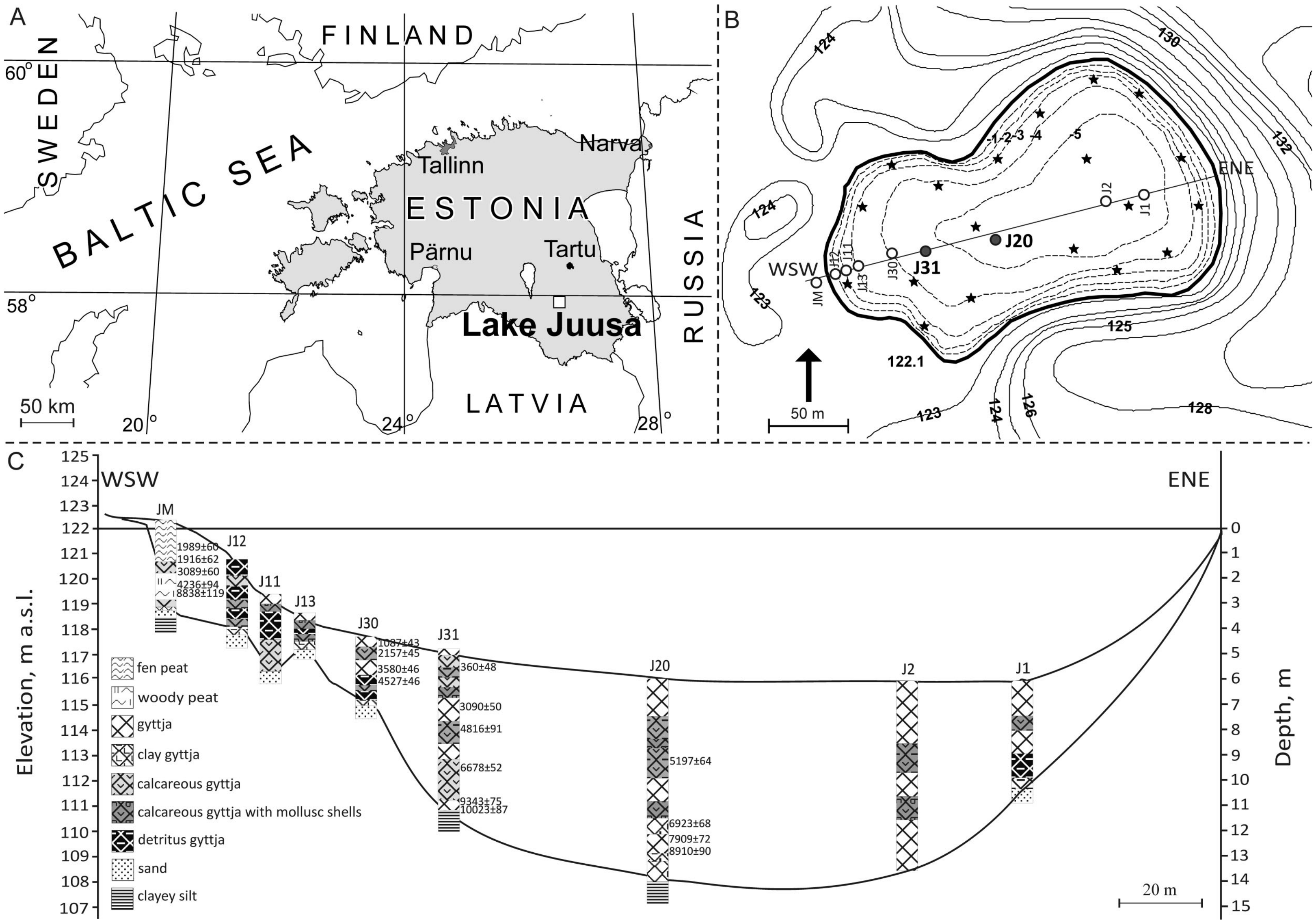

Fig. 1. Study site. **A**, Location of Lake Juusa. **B**, Height contours around the lake and depth contours in the lake. Grey circles denote reference cores (J20, J31), white circles denote additional cores (JM, J12, J11, J13, J30, J2, J1), stars denote surface sediment samples. **C**, Sediment cores, their lithological description and C^{14} data (BP) along the profile WSW–ENE based on Punning et al. (2005b).

Laboratory analyses

All sediment samples from long cores (J20 and J31) and the surface sediment layer were analysed for water, organic and mineral matter content. The content of dry matter in the sediment was determined by drying the samples at 105 °C to constant weight. Organic matter was measured as loss on ignition (LOI) after heating the samples at 550 °C for 3.5 h. The $CaCO_3$ content was calculated as the loss of weight after burning the LOI residue at 950 °C for 2.5 h. The calculations were made according to commonly used standard methods (Bengtsson & Enell 1986; Heiri et al. 2001).

The grain size composition of the sediment samples was determined by wet sieving. Four metallic woven mesh sieves (36, 63, 100 and 315 µm) were stacked vertically and placed in a Vibratory Sieve Shaker 'Analysette 3' PRO. A pre-weighed subsample of the sediment was placed into the upper sieve and, after a suitable period of shaking (generally 15–20 min), the content of each sieve was dried at 105 °C and weighed (Folk 1980; Konert & Vandenberghe 1997; Last 2001). The particle size partitioning was determined from the amount of sediment remaining in each specific sieve, using standard LOI methodology described in the previous paragraph.

Chronology, cartographic analysis and palaeoreconstructions

Detailed data from a comprehensive analysis of cores J20 and J31 (Fig. 1B) and the age–depth curve of the dated cores have been published by Punning et al. (2005b). The cores were dated with the AMS ^{14}C technique – five datings from core J20 and six from core J31. In Table 1 the radiocarbon dates obtained by the AMS method are also given in calibrated years (cal. yr BP) revised by Puusepp (2011), calculated with IntCal09 (Reimer et al. 2009) in OxCal v4.1.3 (Bronk Ramsey 2009). Hereafter all dates are given in conventional ^{14}C years before present (BP) for better comparison with previously published data. The radiocarbon data and lithology of the cores were used to correlate cores with each other.

Cartographic analysis, visualization and digital elevation models of the lake bottom topography were made with MapInfo Professional and VerticalMapper. To analyse temporal and spatial changes in bottom topography, GIS-based databases and 3D digital elevation models of the development phases of the lake were created for 9000 BP, 8000 BP, 4000 BP, 2000 BP and the present. The TIN method with 174 data points was employed for interpolation of the 3D digital elevation models. Based on the compiled 3D digital elevation models, characteristics of the state of the palaeolake were estimated (see Table 2). To analyse the impact of changing slope inclinations on the sedimentation environment in the course of water-level changes, 60° sectors around sites J20 and J31 were used. The sampling site served as the starting point for each sector directed towards the nearest shore in two directions. The slope inclinations for every depth interval within these sectors were calculated from the digital elevation models and used to describe the lake basin topography in the sampling sites.

Statistical analysis of the data was performed with the programs Microsoft Excel, XLStat and SigmaPlot. Correlation coefficients were classified as strong ($|r| \geq 0.8$), moderate ($0.5 < |r| < 0.8$) or weak

Table 1. Radiocarbon and calibrated dates of cores J20 and J31. The dates were calibrated, using IntCal09 (Reimer et al. 2009) in OxCal v4.1.3 (Bronk Ramsey 2009), based on Punning et al. (2005b) and Puusepp (2011)

Core	Depth, cm	Dated material	Laboratory number	^{14}C date yr BP	Calibrated year range (2 δ; 95.4%)
J20	236–237	Charcoal	Erl-8006	2 562 ± 113	2 865–2 350 cal yr BP
	454–456	*Betula* seeds	Erl-5812	5 197 ± 64	6 129–5 880 cal yr BP
	773–775	*Betula* wood	Erl-5813	6 923 ± 68	7 875–7 622 cal yr BP
	876–877	*Betula* seeds	Erl-5814	7 909 ± 72	8 995–8 587 cal yr BP
	923–925	Wood	Erl-5815	8 910 ± 90	10 230–9 732 cal yr BP
J31	98–102	*Pinus* needles	Erl-5941	360 ± 48	501–313 cal yr BP
	321–325	Charcoal	Erl-5942	3 090 ± 50	3 405–3 205 cal yr BP
	430–435	*Betula* seeds	Erl-5943	4 816 ± 91	5 734–5 435 cal yr BP
	601–605	*Betula* seeds	Erl-5944	6 678 ± 52	7 624–7 459 cal yr BP
	811–815	*Pinus* needles	Erl-5945	9 343 ± 75	10 739–10 294 cal yr BP
	861–865	*Betula* seeds	Erl-5946	10 023 ± 87	11 827–11 250 cal yr BP

Table 2. Characteristics of the reconstructed phases of the lake basin (shape factor and dynamic ratio are calculated according to the Håkanson & Jansson 1983)

Characteristic	9000 BP	8000 BP	4000 BP	2000 BP	Present
Water volume, m^3	321 000	20 000	84 000	154 000	111 000
Sediment volume, m^3	–	26 000	69 000	83 000	110 000
Area, m^2	54 400	8 300	25 000	37 100	29 900
Water level, m a.s.l.	124.3	111.9	119.1	122.6	122.1
Sediment surface*, m a.s.l.	107.7	108.2	113.4	115.2	117
Maximum depth, m	16.8	3.7	5.4	7.4	6.0
Average depth, m	5.9	2.5	3.3	4.2	3.7
Maximum length, m	320	150	240	300	250
Maximum width, m	260	90	150	170	160
Average slope inclination, %	13.2	11.2	9.3	9.3	8.7
Shape factor	0.95	0.41	0.54	0.59	0.49
Dynamic ratio	0.04	0.037	0.048	0.046	0.043
Perimeter, m	1 000	400	670	920	700

* Sediment surface is calculated for site J20.

($|r| \leq 0.5$); if $p < 0.05$; n means number of data-points used in analysis.

To describe the sediment limits and bottom topography of the sedimentation zones, a composite parameter (CP) (Terasmaa 2005a, 2005b) was used. The CP is a dimensionless unit that enables differentiation of sedimentation zones and comparison of lakes with different shapes and sizes according to a limited number of parameters describing the lake bottom topography and location of the sampling sites (water depth, slope inclinations and distance from the shore):

$$\mathrm{CP} = \sqrt{\frac{\mathrm{D_r} \times \mathrm{SI_r}}{\mathrm{DS_r}}} = \sqrt{\frac{\sqrt{\mathrm{D} \times \frac{\mathrm{D_{max}}}{\mathrm{D_{average}} \times 3}} \times \sqrt{\mathrm{SI}}}{\sqrt{\frac{\mathrm{DS} \times \mathrm{L}}{\mathrm{R_A} \times \mathrm{W}}}}},$$

where D_r is the relative depth at the sampling site, D is the water depth at the sampling site (m) and $D_{average}$ is the average depth of the lake (m) (the quotient of the maximum depth to the average depth multiplied by 3 is, according to Håkanson & Jansson (1983), the so-called form factor V_d^{-1}), SI_r is the relative slope inclination at the sampling site, SI is the mean slope inclination in the area with a diameter of 6 m surrounding the sampling site (%), DS_r is the relative distance of the sampling site from the shore, DS is the distance from the sampling site to the nearest shore (m), L is the maximum length of the lake (m), R_A is the radius of a circle having an equal area with the lake (m) and W is the maximum width of the lake (m).

To estimate the distribution of areas with different sedimentation regimes in the lake with the use of the CP, a 30 m grid was created on the digital elevation model of each time slice. From the grid the depth, distance from the shore and slope inclinations of every point were found. Slope inclination was determined as the mean value for an area with a diameter of 6 m surrounding the sampling site to reduce the effect of possible random variations in the course of interpolation on the determination of slope inclinations. After the calculation of CP values the Mapinfo and VerticalMapper programs were used to delimit areas with different sedimentation regimes. With the help of the CP it is possible to estimate whether a certain spot in the lake sediment surface is situated in an accumulation or erosion zone: $\mathrm{CP} < 2$ means the accumulation area, $2 < \mathrm{CP} < 3$ means the transition area and $\mathrm{CP} > 3$ means the erosion area (Terasmaa 2005a, 2005b).

RESULTS AND DISCUSSION

Dynamics of palaeolake basins

As has been shown earlier (Punning et al. 2005b), the water level in Lake Juusa has undergone significant fluctuations during the Holocene. Using these data and the 3D models, the sedimentation rate (Fig. 2) and the topographic characteristics of the lake at different time periods (Fig. 3, Table 2) were calculated. In the course of the lake infilling the inclinations of shore slopes decreased, so that the slopes flattened continuously (Fig. 3D) and the sedimentation regime became more strongly affected by sediment erosion in the nearshore area.

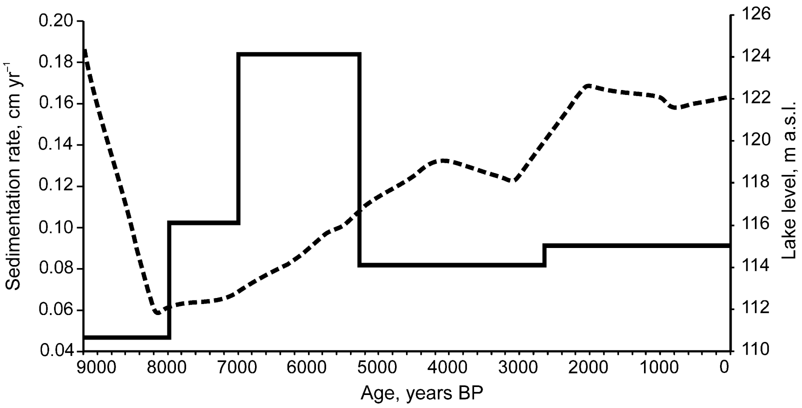

Fig. 2. Dynamics of the sedimentation rate in core J20 (solid line) and water-level changes (dotted line).

At the beginning of the Holocene, about 10 000–9500 BP, the water level was highest and water flooded wide surrounding areas. Around 9000–8000 BP, a sudden drop of the lake level took place and roughly 8000–7500 BP the lake level fell to its minimum. A similar pattern in water-level changes is noted in other lakes in northern Europe and on the territory of the former Soviet Union (Yu & Harrison 1995; Yu 1998). Some of the previously studied lakes in Estonia (e.g. Saarse & Harrison 1992) had an intermediate water level and some a low water level at the beginning of the Holocene. There are no systematic and explainable differences between these two groups. Lake Juusa is acting similarly to lakes Päidre, Punso and Raigastvere (Saarse & Harrison 1992).

Since that time the water level of Lake Juusa has increased continuously to the present level, with the exception of a short period about 3000 BP (Fig. 2); this dry period around 4000–3000 BP is also noted in other lakes (Saarse & Harrison 1992; Yu & Harrison 1995). Digerfeldt (1986) showed that the climate was rather dry around 9000 BP in southern Sweden, but the humidity increased markedly during the early Atlantic period between 8000 and 6400 BP, which caused a water-level rise. The same tendency has been noted by a number of researchers (e.g. Saarse & Harrison 1992; Yu & Harrison 1995; Dearing 1997; Eronen et al. 1999; Ojala & Saarinen 2002; Punning et al. 2007b).

At 10 000–9000 BP, a large area to the west and southwest of the lake was flooded. The settling of fine-grained matter sealed the basin floor and decreased sediment permeability. At the end of the Preboreal period, the lake level stabilized at some 124–125 m a.s.l. (roughly 8 m below the current level, Fig. 3B). The lake basin was steeply sloped (average inclination 13.2%, Table 2), and the hypsographic curve became convex (Fig. 3C). On average, slope inclinations in the 1–4 m depth area were up to 15%, indicating an increase in the erosion zone (Håkanson & Jansson 1983) (Fig. 4). The slopes around site J20 were much steeper than around J31 throughout the Holocene.

Around 8000 BP, when the lake level fell to its minimum, the area of the lake was less than 1 ha. The average slope inclination decreased to 11.2% and the lake hypsographic curve was linear or slightly concave (Fig. 3D). The lake level was then lower than the sediment basin in site J31, suggesting the entrainment of previously deposited sediments at that time. Changes in the lake level caused changes in the sedimentation rate (Fig. 2). The most significant expansion of the accumulation zone started immediately after the deep drop of the lake level at 8200–8000 BP. The subsequent increase in the lake level caused intensive erosion from the surrounding slopes and the sedimentation rate reached its maximum around 6500–5000 BP.

The lake level reached its first peak (see Fig. 2, Table 2) at 4000 BP. The average slope inclination was then 9.3% and the hypsographic curve became linear. Considering the composition of basal sediments, it seems that evaporation and infiltration might have exceeded precipitation at that time, leading to a negative hydrological balance in the lake and a reduced water level. Another slight increase in the lake level (up to 4 m) took place between 3000 and 2000 BP. The average slope inclination of the lake was then 9.3% and the lake level reached its maximum. Shore erosion probably increased and the lake hypsographic curve became convex in the nearshore area and approximately linear in the deepest part of the lake. The slopes in the erosion area around site J20 had much higher values than lake average (Fig. 4), mainly because of steeper slopes in the northern part of the lake.

About 2000–1000 BP, the lake water level exceeded the present level. Shortly thereafter, a rapid decrease was followed by a continuous increase, which brought the lake level up to the current state. At present, the lake

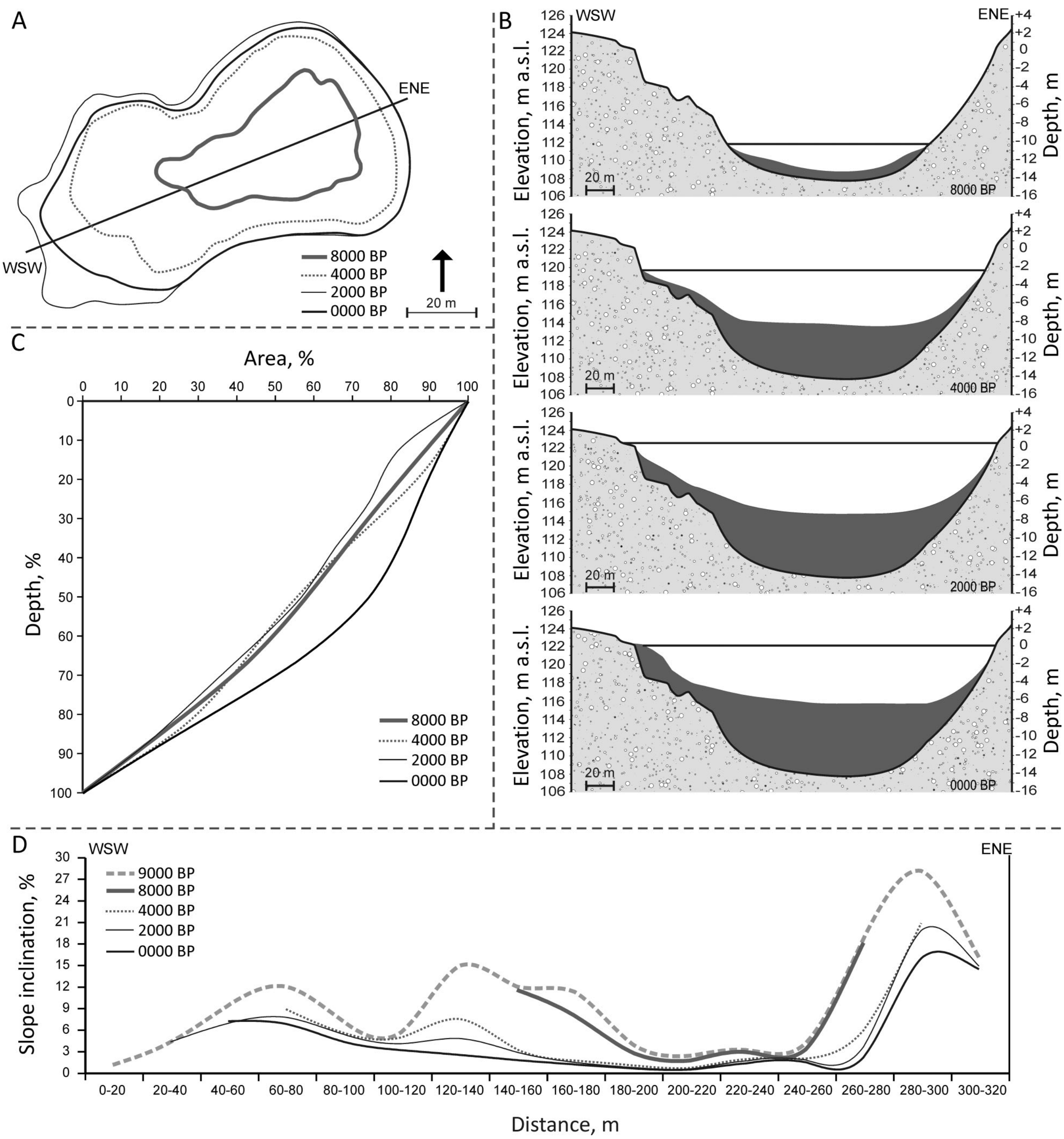

Fig. 3. Reconstructed palaeobasins of Lake Juusa (at 8000 BP, 4000 BP, 2000 BP and 0000 BP). **A**, Shoreline; **B**, cross-sections (SW–NE) (left axis: elevation above sea level, right axis: water depth relative to current lake level); **C**, hypsographic curves; **D**, changes in the average slope inclination on a 10 m wide cross section (location of the profile is shown in **A**).

sediment surface topography and slope inclinations are similar to those prevailing at 4000 BP (Fig. 3D) (excluding the deeper part where, due to progressive infilling, the slopes have smaller inclinations), the average slope inclination in the lake is 8.7%, the hypsographic curve is concave, the nearshore area deepens abruptly and the deepest part of the lake is flat and gently sloping.

Dynamics of the sedimentation zones

Detailed analysis of changes in the lake topography makes it possible to describe changes in the spatial distribution of sedimentation zones in the lake basin. The CP was used to reconstruct the limits of different zones within the lake (Terasmaa 2005b). In the sediment

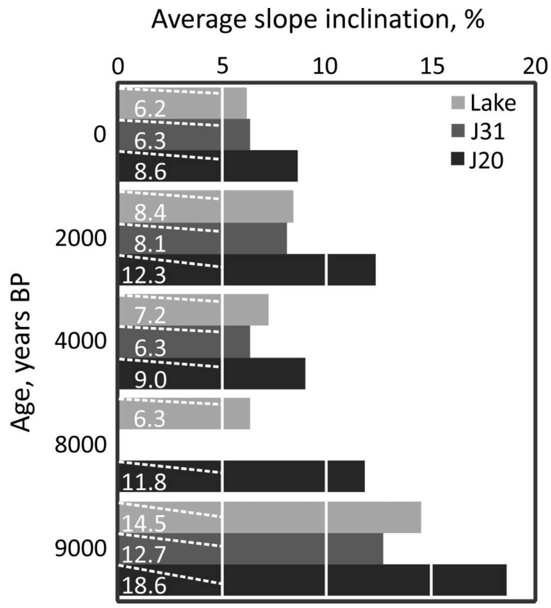

Fig. 4. Average slope inclination in the entire lake littoral zone (water depth up to 4 m) and in the 60 degree sectors directing from sampling sites to the nearest shore (at 8000 BP J31 values are missing because of low water level). The dotted white line denotes inclination in per cent of the length of the line.

surface where the CP values are less than two, sediment accumulation dominates. The CP values from two to three are typical of transition zones, and areas with CP values higher than three are considered as erosion zones (Fig. 5).

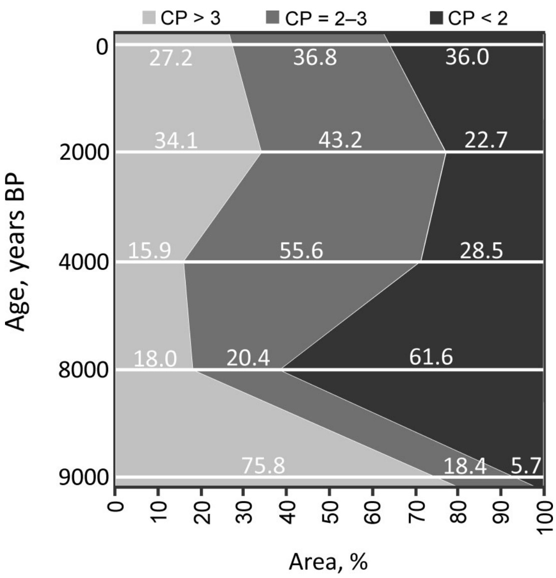

Fig. 5. Composite parameter (CP) (Terasmaa 2005b) values for the palaeolake basins. Values are calculated relative to every palaeolake basin. CP > 3: erosion area; CP = 2–3: transition area; CP < 2: accumulation area.

According to the CP values, at 9000 BP an erosion zone was dominant throughout the lake, excluding a small central area. Although the nearshore region was gentle and shallow, the deeper part of the lake was steeply sloped (Fig. 3D). During the infilling and water-level rise, the size of the accumulation zone increased. At 8000 BP, when the lake area was smallest and the average slope inclination of the lake was relatively small, more than 60% of the lake bottom acted as an accumulation zone (Fig. 5). In the course of the lake-level rise from 8000 to 4000 BP, the proportion of the accumulation zone continuously decreased. The transition zone increased and remained around 40–50% of the lake area. Thus, the transition zone, where sedimentation conditions are most variable, is dominant in the lake. Throughout the Holocene (with the exception of 8000 BP), reference site J31 remained in the transition zone.

Sediment textural changes

The lithological composition of the surface sediments of Lake Juusa shows that the content and grain size of particles are the highest in the nearshore zones in the eastern and northeastern parts of the lake where slope inclinations are the highest.

The water-level fluctuations in Lake Juusa initiated a comprehensive reworking of material deposited earlier. As the correlation of the sediment sequences shows, sediments most likely accumulated also near the shore during the regressive period and were subsequently eroded and redeposited during the transgressive period (Punning et al. 2005a). Resedimentation during transgression–regression cycles disturbed the primary stratigraphic sequence of sediments. Sediments accumulating during the transgressive–regressive period originate from two main sources: within-lake reworking of concurrently accumulated sediments and erosion of nearshore glacial sediments, as was demonstrated previously in Lake Martiska (Terasmaa 2005b; Punning et al. 2007a, 2007b).

The lithological composition of the sediments accumulated in cores J31 and J20 show similar patterns (Fig. 6). At 10 000–9000 BP fine-grained sediments (mainly silt) dominated in both studied cores. The lake-level drop ca 8000 BP is reflected in both cores by a conspicuous increase in the influx of coarser material, which implies that the coring sites were close to the erosion area. An increase in the ratio of organic carbon to nitrogen (OC/N) suggests that the increased share of organic matter originated either from autochthonous macrophytes or from the catchment (Punning & Tõugu 2000).

During the transgression after 8000 BP, the proportion of coarse-grained matter in both cores decreased, most notably in core J20. In response to the lake-level rise,

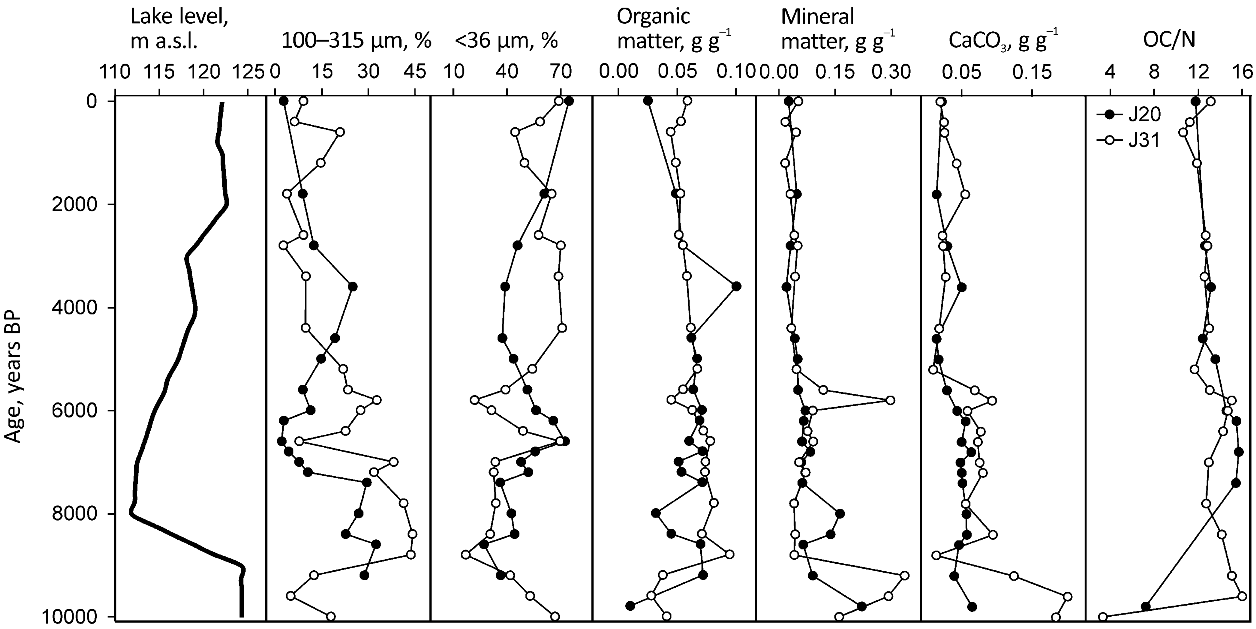

Fig. 6. Lake-level changes and sediment lithology in cores J20 and J31. OC/N, organic carbon to nitrogen ratio.

the erosion area extended and the accumulation rate increased. As the distance from the shore increased, the influx of fine-grained material around sites J20 and J31 also increased and reached its highest values roughly at 6600 BP. Around 6000 BP, an extreme event in the sedimentation environment took place. This event is documented in core J31 as a sharp short-term increase in coarse-grained material. In core J20, taken from a location further from the nearest shore, the same tendency can be noted, though on a much smaller scale. Sharp changes in this period can also be identified in the composition of dry matter (Fig. 6). These changes show that the main mineral influx was from the shores with lower inclinations.

The present-day limit between the accumulation and erosion zones in Lake Juusa can be drawn at a depth of 3–4 m (Terasmaa 2005a). As our analysis of reconstructed palaeobasins showed, the water depth exceeded this depth in the study site J20 at 5500–5000 BP. In core J31, this milestone was reached later, around 4000 BP.

The subsequent lake-level rise brought about changes in the slope inclinations in the erosion zone. When the water level reached the limit of sediments that had accumulated during the transgression in the Late Holocene (at a level of about 118 m a.s.l.), the erosion of outwashed and coarser-grained sediments began. There is an apparent contradiction between the textures of sediments in the studied cores about 5000 BP: the proportion of coarser material is higher in the profundal (J20) than in the littoral (J31) core (Figs 3, 6). The differences in the slope inclinations (see Fig. 4) explain the differences in the sedimentation environments between these two cores.

Changes in the sedimentation environment

The dynamics of the lake-level changes can be roughly separated into two periods: from 10 000 BP until about 6600 BP and from 6600 BP until the present. Correlation analysis confirms that if we split the data into two groups, the relationships between sediment characteristics will be stronger, especially in the case of core J31 (Table 3). Over the whole sequence (10 000–0 BP) there are only three statistically significant correlations between different characteristics.

In the lower part of core J31 (accumulated from 10 000 to 6600 BP) five statistically significant correlations between sediment characteristics were observed. Moderate positive correlations were found between lake-level fluctuations and the composition of mineral matter, and between the content of mineral matter and $CaCO_3$. A moderate negative correlation was found between the coarser material (100–315 µm) and mineral matter ($r = -0.78$, $p = 0.013$, $n = 9$) (and a positive correlation with the content of organic matter). Such relationship is somewhat unusual; normally, small lakes show a decrease in organic compounds and an increase in mineral compounds with a rise in the proportion of coarser material (Terasmaa 2005b). The reverse relationship can be partly explained by the coincidence

Table 3. Statistically significant correlations ($p < 0.05$) between sediment composition characteristics and lake level. Min, mineral matter; OC/N, organic carbon to nitrogen ratio

J31

10 000–0 BP	*r* value ($n = 24$)
100–315 (μm) vs <36 (μm)	−0.86
100–315 (μm) vs lake level (m a.s.l.)	−0.54
Min (g g^{-1}) vs $CaCO_3$ (g g^{-1})	0.74

10 000–6600 BP	*r* value ($n = 9$)
100–315 (μm) vs <36 (μm)	−0.82
100–315 (μm) vs min (g g^{-1})	−0.78
100–315 (μm) vs $CaCO_3$ (g g^{-1})	−0.69
Min (g g^{-1}) vs $CaCO_3$ (g g^{-1})	0.73
Min (g g^{-1}) vs lake level (m a.s.l.)	0.74

6600–0 BP	*r* value ($n = 15$)
100–315 (μm) vs <36 (μm)	−0.91
100–315 (μm) vs min (g g^{-1})	0.67
100–315 (μm) vs lake level (m a.s.l.)	−0.55
100–315 (μm) vs OC/N	0.53
<36 (μm) vs $CaCO_3$ (g g^{-1})	−0.57
<36 (μm) vs min (g g^{-1})	−0.68
Min (g g^{-1}) vs $CaCO_3$ (g g^{-1})	0.72
Min (g g^{-1}) vs OC/N	0.59
Min (g g^{-1}) vs lake level (m a.s.l.)	−0.56
$CaCO_3$ (g g^{-1}) vs lake level (m a.s.l.)	−0.61
OC/N vs lake level (m a.s.l.)	−0.70

J20

10 000–0 BP	*r* value ($n = 19$)
100–315 (μm) vs <36 (μm)	−0.89
Min (g g^{-1}) vs $CaCO_3$ (g g^{-1})	0.60
Min (g g^{-1}) vs OC/N	−0.49
OC/N vs lake level (m a.s.l.)	−0.63

10 000–6600 BP	*r* value ($n = 10$)
100–315 (μm) vs <36 (μm)	−0.90
Min (g g^{-1}) vs $CaCO_3$ (g g^{-1})	0.64
Min (g g^{-1}) vs OC/N	−0.73
OC/N vs lake level (m a.s.l.)	−0.64

6600–0 BP	*r* value ($n = 9$)
100–315 (μm) vs <36 (μm)	−0.91
Min (g g^{-1}) vs OC/N	0.83
Min (g g^{-1}) vs lake level (m a.s.l.)	−0.72
OC/N vs lake level (m a.s.l.)	−0.74

of various factors, such as transgression, which brought about heavier erosion of mineral material and an increasing content of organic matter. Those changes are also confirmed by changes in the sedimentation rates (Fig. 2). During 10 000–6600 BP, the accumulation zone expanded faster than the water table rose, reaching its highest values around 6000 BP, when the sediment area comprised over 50% of the lake area.

The upper part of core J31 (accumulated from 6600 BP to the present) showed 11 statistically significant correlations between sediment characteristics, and some of them have an opposite sign as compared to the previous period (Table 3). The composition of mineral matter shows a moderate positive correlation with the share of coarse-grained material and a negative correlation with the share of fine-grained material (respectively $r = 0.67$, $p = 0.006$, $n = 15$ and $r = -0.68$, $p = 0.005$, $n = 15$). Such relationships are in accordance with the data obtained in a study of surface sediment in Lake Juusa (Terasmaa 2005b), where the contents of fine-grained material and organic matter in the surface layer have strong or moderate positive correlations. Correlations between other parameters follow the same tendency. Therefore it seems that the majority of the changes in the sediment composition were connected with lake-level changes. An expansion of the lake area led to a decreasing rate of accumulation of coarser material and an increasing rate of organic matter accumulation in the central area of the lake. Simultaneously, the limit of the accumulation zone moved outwards and the slope inclinations decreased. Due to those processes there was not enough energy to transport larger particles from the nearshore area to the central part of the lake. Thus, even in core J31, the proportion of particles of 100–315 μm size fell to less than 10% in total weight. At the same time, the sedimentation rate decreased (Fig. 2), mainly due to the larger accumulation zone area (Fig. 5).

The existing statistically significant correlations between different variables in core J20 are similar to those in core J31, however somewhat weaker. This suggests that the sedimentation pattern in core J20 was more stable and that this site had primarily been in the accumulation zone.

CONCLUSIONS

Reconstruction of the development of the Lake Juusa basin during the Holocene with the help of the 3D digital elevation models, compiled for the palaeolake stages at 9000 BP, 8000 BP, 4000 BP, 2000 BP and the present, gives a better understanding of the very complex system. By combining lithological (mineral and organic matter, grain size) information from sediment cores with 3D digital elevation models it is possible to describe lake basin development and to estimate changes in the sedimentation patterns during the regressive and transgressive stages of the water level.

The results obtained from the study of the surface sediments and sediment cores J20 and J31 from Lake Juusa allowed us to quantify several parameters connected with lake basin development, which affect the sediment accumulation pattern in small lakes – slope inclinations, water depth, distance from the shore. With the help of the composite parameter (CP) it was possible to allocate the spatial changes in sediment accumulation and erosion zones. In Lake Juusa, the accumulation zone was largest during the regression phase (around 8000 BP) and smallest at 2000 BP. As the correlation of the sediment sequences shows, sediments most likely accumulated near the shore during the regressive period and were subsequently eroded and redeposited during the transgressive period. When the water level reached the limit of sediments that had accumulated during the transgression in the Late Holocene, the erosion of outwashed and coarser-grained sediments began.

The lithological compositions of sediments in cores J31 and J20 show similar patterns. At 10 000–9000 BP fine-grained sediments dominated in both cores. The water-level decrease at 8000 BP is reflected in a conspicuous increase in the influx of coarser material. During the transgression after 8000 BP, the proportion of coarse-grained matter in both cores decreased, as the distance from the shore increased. Around 6000 BP, an extreme event in the sedimentation environment took place, which is documented as a sharp short-term increase in coarse-grained material in core J31; in core J20 the same tendency can be noted on a much smaller scale. The present-day limit between the accumulation and erosion zones in Lake Juusa (at a depth of 3–4 m) was exceeded in the study site J20 at 5500–5000 BP, in core J31 around 4000 BP. There is an apparent contradiction between the texture of sediments in the studied cores about 5000 BP: the proportion of coarser material is higher in the profundal J20 than in the littoral J31 – this difference can be explained by differences in slope inclinations. Consequently, not only are water-level fluctuations evident in the sediment grain-size distribution, but sites located spatially rather close to each other commonly have significantly different sedimentation patterns.

The results obtained in this study show that, in order to understand lake basin evolution and water-level changes, the sampling sites should be selected close to the transitional zone and more than one core from a lake is needed. Three-dimensional digital elevation models of lake basins are useful tools for visualizing data and for hypothesizing about possible effects of lake-level fluctuations on the lake as a system. The results suggested that we have to consider palaeolake stages as completely different lakes with different sedimentation patterns – the hypsographic curve of Lake Juusa was convex at the beginning of the Holocene and is concave nowadays. The share of the accumulation areas varied from 6% to 60% at the beginning of the Holocene and is around 30% nowadays. By constructing lake basins for different stages in the development of Lake Juusa and applying knowledge from surface sediment studies to long core studies, it was possible to describe the lake development during the Holocene in a more detailed way and to clarify the impact of water-level changes on the sedimentation environment. Possibilities of similar changes in the sedimentation pattern and influence of lake basin development should be considered in every interpretation and conclusion in palaeolimnological studies.

Acknowledgements. The aim and research problems for this paper were formulated together with the late Prof. J.-M. Punning, who also greatly contributed to the writing of the preliminary version of the paper. The study was supported by the Estonian Ministry of Education and Research (targeted financed project SF0280016s07) and the Estonian Science Foundation (grant 6857). The author is grateful to colleagues for participating in the fieldwork and discussions, to John F. Boyle for helping to improve the language and to clarify ideas in an earlier version of the manuscript and to Docent Jaan Jõgi for helpful comments. The reviewers (Wim Hoek and Mikael Malmaeus) are acknowledged for their suggestions.

REFERENCES

Allen, J. R. L. 1985. *Principles of Physical Sedimentology*. George Allen and Unwin, Boston, 272 pp.

Bengtsson, L. & Enell, M. 1986. Chemical analysis. In *Handbook of Holocene Palaeoecology and Palaeohydrology* (Berglund, B. E., ed.), pp. 423–451. John Wiley & Sons, Chichester–New York.

Blais, J. M. & Kalff, J. 1995. The influence of lake morphometry on sediment focusing. *Limnology and Oceanography*, **40**, 582–588.

Boyle, J. F. 2001. Inorganic geochemical methods in palaeolimnology. In *Tracking Environmental Change Using Lake Sediments. Volume 2 – Physical and Geochemical Methods* (Last, W. M. & Smol, J. P., eds), pp. 83–141. Kluwer Academic Publishers, London.

Bronk Ramsey, C. 2009. Bayesian analysis of radiocarbon dates. *Radiocarbon*, **51**, 337–360.

Davis, M. B. & Ford, M. S. 1982. Sediment focusing in Mirror Lake, New Hampshire. *Limnology and Oceanography*, **27**, 137–150.

Dearing, J. A. 1997. Sedimentary indicators of lake-level changes in the humid temperate zone: a critical review. *Journal of Paleolimnology*, **18**, 1–14.

Digerfeldt, G. 1986. Studies on past lake-level fluctuations. In *Handbook of Holocene Palaeoecology and Palaeohydrology* (Berglund, B. E., ed.), pp. 127–143. John Wiley and Sons, Chichester–New York.

Eronen, M., Hyvärinen, H. & Zetterberg, P. 1999. Holocene humidity changes in northern Finnish Lapland inferred from lake sediments and submerged Scots pines dated by tree-rings. *The Holocene*, **9**, 569–580.

Folk, R. L. 1980. *Petrology of Sedimentary Rocks*. Hemphill Publishing Company, Austin, Texas, 184 pp.

Gilbert, R. 2003. Spatially irregular sedimentation in a small, morphologically complex lake: implication for paleoenvironmental studies. *Journal of Paleolimnology*, **29**, 209–220.

Håkanson, L. & Jansson, M. 1983. *Principles of Lake Sedimentology*. Springer-Verlag, Berlin, 315 pp.

Hannon, G. E. & Gaillard, M.-J. 1997. The plant–macrofossil record of past lake-level changes. *Journal of Paleolimnology*, **18**, 15–28.

Heiri, O., Lotter, A. F. & Lemcke, G. 2001. Loss on ignition as a method for estimating organic and carbonate content in sediments: reproducibility and comparability of results. *Journal of Paleolimnology*, **25**, 101–110.

Jaagus, J. & Tarand, A. 1988. Sademete territoriaalne jaotus Eestis [Territorial distribution of precipitation in Estonia]. *Yearbook of the Estonian Geographical Society*, 24, 5–18 [in Estonian].

Kangur, M., Koff, T., Punning, J.-M., Vainu, M. & Vandel, E. 2009. Lithology and biostratigraphy of the Holocene sediment sequence in L. Ķūžu, Vidzeme Heights (Central Latvia). *Geological Quarterly*, **53**, 199–208.

Koff, T., Punning, J.-M., Sarmaja-Korjonen, K. & Martma, T. 2005. Ecosystem responses to early and late Holocene lake-level changes in Lake Juusa, southern Estonia. *Polish Journal of Ecology*, **53**, 553–570.

Konert, M. & Vandenberghe, J. 1997. Comparison of laser grain size analysis with pipette and sieve analysis: a solution for the underestimation of the clay fraction. *Sedimentology*, **44**, 523–535.

Last, W. M. 2001. Mineralogical analysis of lake sediments. In *Tracking Environmental Change Using Lake Sediments. Volume 2 – Physical and Geochemical Methods* (Last, W. M. & Smol, J. P., eds), pp. 143–187. Kluwer Academic Publishers, London.

Lehman, J. T. 1975. Reconstructing the rate of accumulation of lake sediment: the effect of sediment focusing. *Quaternary Research*, **5**, 541–550.

Magny, M., Begeot, C., Guiot, J., Marguet, A. & Billaud, Y. 2003. Reconstruction and palaeoclimatic interpretation of mid-Holocene vegetation and lake-level changes at Saint-Jorioz, lake Annecy, French Pre-Alps. *The Holocene*, **13**, 265–275.

Nesje, A. & Dahl, S. O. 2001. The Greenland 8200 cal. yr BP event detected in loss-on-ignition profiles in Norwegian lacustrine sediment sequences. *Journal of Quaternary Sciences*, **16**, 155–166.

Ojala, A. E. K. & Saarinen, T. 2002. Paleosecular variation of the earth's magnetic field during the last 10 000 yr based on an annually laminated sediment of Lake Nautajärvi, central Finland. *The Holocene*, **12**, 391–400.

Punning, J.-M. & Tõugu, K. 2000. C/N ratio and fossil pigments in sediments of some Estonian lakes: an evidence of human impact and Holocene environmental change. *Environmental Monitoring and Assessment*, **64**, 549–567.

Punning, J.-M. & Puusepp, L. 2007. Diatom assemblages in sediments of Lake Juusa, Southern Estonia with an assessment of their habitat. *Hydrobiologia*, **586**, 27–41.

Punning, J.-M., Terasmaa, J., Koff, T. & Alliksaar, T. 2003. Seasonal fluxes of particulate matter in a small closed lake in northern Estonia. *Water, Air and Soil Pollution*, **149**, 77–92.

Punning, J.-M., Puusepp, L. & Koff, T. 2004. The spatial variability of diatoms, subfossil macrophytes and OC/N values in surface sediments of Lake Väike Juusa (southern Estonia). *Proceedings of the Estonian Academy of Sciences, Biology, Ecology*, **53**, 147–160.

Punning, J.-M., Terasmaa, J. & Kadastik, E. 2005a. Grain size of the bottom sediments of Lake Juusa (southern Estonia) as the indicator of water level fluctuations. *Proceedings of the Estonian Academy of Sciences, Geology*, **54**, 40–51.

Punning, J.-M., Koff, T., Kadastik, E. & Mikomägi, A. 2005b. Holocene lake level fluctuations recorded in the sediment composition of Lake Juusa, southeastern Estonia. *Journal of Paleolimnology*, **34**, 377–390.

Punning, J.-M., Koff, T., Sakson, M. & Kangur, M. 2007a. Holocene pattern of organic carbon accumulation in a small lake in Estonia. *Polish Journal of Ecology*, **55**, 5–14.

Punning, J.-M., Boyle, J. F., Terasmaa, J., Vaasma, T. & Mikomägi, A. 2007b. Changes in lake sediment structure and composition caused by human impact: repeated studies of Lake Martiska, Estonia. *The Holocene*, **17**, 145–151.

Puusepp, L. 2011. *Spatio-Temporal Variability of Diatom Assemblages in Lake Sediments*. Dissertation on Natural Sciences 24, Tallinn University, 142 pp.

Reimer, P. J., Baillie, M. G. L., Bard, E., Bayliss, A., Beck, J. W., Blackwell, P. G., Bronk Ramsey, C., Buck, C. E., Burr, G. S., Edwards, R. L., Friedrich, M., Grootes, P. M., Guilderson, T. P., Hajdas, I., Heaton, T. J., Hogg, A. G., Hughen, K. A., Kaiser, K. F., Kromer, B., McCormac, F. G., Manning, S. W., Reimer, R. W., Richards, D. A., Southon, J. R., Talamo, S., Turney, C. S. M., van der Plicht, J. & Weyhenmeyer, C. E. 2009. IntCal09 and Marine09 radiocarbon age calibration curves, 0–50,000 years cal BP. *Radiocarbon*, **51**, 1111–1150.

Reintam, L. 1995. Muldade kujunemine [Formation of the soils]. In *Eesti. Loodus* (Raukas, A., ed.), pp. 419–429.

Valgus, Eesti Entsüklopeediakirjastus, Tallinn [in Estonian].

Richard, B., Renberg, I. & Brännvall, M. L. 2001. A whole-basin study of sediment accumulation using stable lead isotopes and fly-ash particles in an acidified lake, Sweden. *Limnology and Oceanography*, **46**, 176–187.

Saarse, L. & Harrison, S. P. 1992. Holocene lake-level changes in the eastern Baltic region. In *Estonia: Man and Nature* (Kaare, T. et al., eds), pp. 6–20. Estonian Academy of Sciences and Estonian Geographical Society, Tallinn.

Snowball, I., Zillén, L. & Gaillard, M.-J. 2002. Rapid early-Holocene environmental changes in northern Sweden based on studies of two varved lake-sediment sequences. *The Holocene*, **12**, 7–16.

Tarasov, P. E. & Harrison, S. P. 1989. Lake status records from the former Soviet Union and Mongolia: a continental-scale synthesis. *Paläoklimaforschung/Palaeoclimate Research*, **25**, 115–130.

Terasmaa, J. 2005a. *Seston Fluxes and Sedimentation Dynamics in Small Estonian Lakes*. Dissertation on Natural Sciences 11, Tallinn University, 199 pp.

Terasmaa, J. 2005b. Bottom topography and sediment lithology in two small lakes in Estonia. *Proceedings of the Estonian Academy of Sciences, Biology, Ecology*, **54**, 171–189.

Terasmaa, J. 2009. 3D digital height models as a tool for reconstructing the impact of lake-level fluctuations on the sedimentation dynamics in a small lake (Southern Estonia). In *Abstract Volume: 11th International Paleolimnology Symposium* (Caballero, M., Ortega, B., Lozano, S., Zarate, P., Rosas, J., Sosa, S. & Rodriquez, A., eds), p. 144.

Yang, H., Rose, N. L., Battarbee, R. W. & Monteith, D. 2002. Trace metal distribution in the sediments of the whole lake basin for Lochnagar, Scotland: a palaeolimnological assessment. *Hydrobiologia*, **479**, 51–61.

Yu, G. 1998. European lake status data base: continental-scale synthesis for the Holocene. *Paläoklimaforschung/Palaeoclimate Research*, **25**, 99–114.

Yu, G. & Harrison, S. P. 1995. Holocene changes in atmospheric circulation patterns as shown by lake status changes in northern Europe. *Boreas*, **24**, 260–268.

Järvenõo arengu mõju settimisdünaamikale Holotseenis Lõuna-Eesti väikejärve näitel

Jaanus Terasmaa

Järvesetted leiavad paleogeograafiliste rekonstruktsioonide koostamisel laialdast kasutust kogu maailmas. Sageli põhinevad sellised kliimat, valgala arengut ja järve veetaseme muutust rekonstrueerivad uuringud ühel puursüdamikul, mis on võetud nüüdisjärve sügavaimast kohast. Settes peituva info korrektseks interpreteerimiseks tuleb esmalt mõista sette kujunemise ajalis-ruumilist dünaamikat ja sedimentatsiooniprotsessi tervikuna. Sette kujunemist mõjutavad mitmed tegurid, millest väikejärvedes võib olulisimateks pidada järvenõo ja settepinna topograafiat ja järve kuju ning suurust. Käesolevas artiklis on rekonstrueeritud Lõuna-Eestis asuva Väike Juusa järve nõo arengulugu Holotseenis ja koostatud kolmemõõtmelised digitaalsed kõrgusmudelid ajaperioodide 9000, 8000, 4000 ning 2000 aastat tagasi ja tänapäeva kohta. Kõrgusmudelite abil on võimalik järvenõo arengudünaamikat detailsemalt vaadelda ja leida settimirežiimi muutused erinevatel ajahetkedel. Tulemused kinnitavad, et sama järve tuleb ajas tagasi minnes käsitleda erineva veekoguna (paleojärvena), kus valitsenud settimistingimused võisid täiesti erinevad olla. Näiteks võis uuritud Väike Juusa järves akumulatsiooniala ulatus varieeruda vahemikus 6–60%, samuti muutus järve batümeetriline kõver järvenõo settega täitumise käigus kumerast nõgusaks. Sellist suurt ajalis-ruumilist muutlikkust tuleb lisaks tulemuste interpreteerimisele arvesse võtta ka proovivõtukoha valikul.